

A Comparative Evaluation of Energy- and Entropy-Stable Summation-by-Parts and Discontinuous Galerkin Methods

Yewon Lee

August 2019

Abstract

Discontinuous Galerkin (DG) and Summation-by-Parts (SBP) methods can be extended to arbitrary orders of accuracy, making them suitable for numerically solving PDEs with high accuracy on a given mesh compared to low-order methods that are used in industry. However, their stability is not guaranteed in theory, especially for nonlinear problems. DG schemes based on entropy variables are nonlinearly stable only with exact integration, while entropy-stable SBP schemes do not rely on exact integration for nonlinear stability. In either case, guaranteeing entropy-stability can be more computationally costly. A more inexpensive alternative of using energy-stable DG and SBP schemes guarantees stability only for linear problems. Given the limitations of our understanding of the performance of energy- and entropy-stable DG and SBP schemes through theory only, it is of interest to assess their performance in practice and determine which stability properties are important for different classes of problems. In our work, an existing computer program is modified to simulate problems with increasing levels of difficulty, using subsets of the following schemes: i) energy-stable DG ii) entropy-stable DG, iii) energy-stable SBP, and iv) entropy-stable SBP. For each scheme, we conduct convergence studies and determine the limiting CFL for stability. Our study demonstrates the performance of energy- and entropy-stable DG and SBP schemes in practice and can serve as a foundation for choosing high-order schemes that meet the cost and stability demands of particular problems.

1 Introduction

High-order methods in computational fluid dynamics (CFD) are capable of delivering high accuracy on a given mesh compared to low-order methods. Discontinuous Galerkin (DG) and Summation-by-Parts (SBP) methods are examples of numerical methods that can be extended to be arbitrarily high-order, defined as third-order or greater [8]. These methods have increasingly gained attention in the CFD research community [8] due to their potential in solving problems that are vortex-dominated. However, their lack of robustness, specifically in terms of guaranteeing nonlinear stability, continues to be a factor that impedes their usage in industry.

Energy-stable DG and SBP methods guarantee stability for linear problems, but they are not guaranteed to be stable for nonlinear problems. Entropy-stable schemes are a potentially more expensive alternative [6] that can guarantee nonlinear stability with limitations. For instance, the proof of nonlinear stability of the entropy-stable DG scheme (more accurately the DG scheme based on entropy variables) requires that integration is exact, which may not be possible in practice. Crean et al. [2] developed an entropy-stable SBP discretization which provably conserves entropy without integral exactness. In either case, a study of the practical performance of each of the four schemes (entropy-stable DG and SBP, and entropy-stable DG and SBP) can inform us of their relative stability, cost, and accuracy in practice. For instance, it would be interesting to see whether the energy-stable schemes can robustly solve nonlinear problems in practice without a theoretical guarantee, especially if they are less computationally costly than entropy-stable schemes.

The goal of our study is to assess and compare the practical performance of energy- and entropy-stable DG and SBP schemes by applying them to a series of problems, and to determine the stability properties that are important for each class of problem in our study. Specifically, we are interested in observing each of the schemes' ability to deliver high accuracy on coarse meshes and to maintain (depending on the problem) linear or nonlinear stability at large time steps, or CFL values. We address these two objectives by conducting convergence studies for each scheme and problem that we study, and by identifying the maximum CFL values for which each of the schemes remain stable. These two pieces of information will allow us to deduce the mesh refinement and time step requirements to meet accuracy and stability requirements, and in turn can also inform us of their approximate computational cost. Through studying the practical performance of energy- and entropy-stable DG and SBP schemes, our study will demonstrate the potential and limitations of each of the schemes that may not be possible to identify through theory only.

2 Roadmap

This report is organized as follows. Section 3 describes the test cases that were studied, identifies the DG and SBP schemes that were used to solve each case, and describes the implementation of the schemes. Section 4 presents and discusses the results from each test case. We conclude the report in Section 5.

3 Test Cases and Methods

This section presents the test cases and the specific schemes that were applied to each test case. Three test cases with increasing levels of difficulty were simulated, where ‘difficulty’ means challenging on the grounds of ensuring stability.

3.1 Linear Advection

In this test case, the one-dimensional linear advection problem

$$\frac{\partial u}{\partial t} = a \frac{\partial u}{\partial x}$$

with $a = 1$ and the following initial condition and analytical solution is solved:

$$u(x, 0) = e^{-0.5[(x-0.5)/0.08]^2}.$$

The problem is solved using periodic boundary conditions on the domain of $[0, 1]$ until $t = 5$. The initial solution propagates to the right and wraps around to $x = 0$ periodically every 1 unit of time. This test case was run to verify that energy-stable DG and SBP schemes were sufficient to ensure linear stability in practice.

Given that this is a linear problem, three energy-stable schemes were tested, including: i) the DG method with an upwind flux, ii) the SBP method with an upwind flux, and iii) the SBP method with a symmetric flux. This test case was used to verify the energy-stable properties of each scheme and find any differences in performance. Details of their implementation are shown in Table 1. Note that a $2p + 1$ quadrature rule was applied with the DG scheme; this ensures that polynomials of degree up to $2p + 1$ are integrated exactly using the quadrature rule, where p refers to the degree of the scheme.

Table 1: Implementation of DG and SBP schemes for the linear advection problem

Scheme (method & flux)	Basis functions	Quadrature/ nodal distribution	Time marching
DG (upwind flux)	Lagrange	Legendre-Gauss, $2p + 1$	RK4
SBP (upwind flux)	N/A	Legendre-Gauss	RK4
SBP (symmetric flux)	N/A	Legendre-Gauss	RK4

3.2 Isentropic Vortex

This test case [6] simulates the propagation of a vortex in compressible inviscid flow. The analytical solution is given by

$$u = 1 - \frac{\alpha}{2\pi}(y - y_0)e^{1-r^2},$$

$$v = \frac{\alpha}{2\pi} (x - (x_0 + t)) e^{1-r^2},$$

$$\rho = \left(1 - \frac{\alpha^2(\gamma - 1)}{16\gamma\pi^2} e^{2(1-r^2)} \right)^{\frac{1}{\gamma-1}},$$

$$p = \rho^\gamma$$

where $r^2 = (x - (x_0 + t))^2 + (y - y_0)^2$, the heat capacity ratio $\gamma = 1.4$, and the vortex strength $\alpha = 3$. The solution is a vortex that propagates from $(x_0, y_0) = (5, 0)$ at initial time to the right until a final time of $t = 5$. The problem is nonlinear, vortex-dominated, and isentropic, making it a suitable test case for assessing nonlinear stability properties and accuracy of schemes. The problem is run on the domain of $[0, 20] \times [-5, 5]$ using periodic boundary conditions on all four sides.

Table 2: Implementation of energy- and entropy-stable DG and SBP schemes for the isentropic vortex problem

Scheme	Basis functions	Quadrature/nodal distribution	Numerical flux	Variable type	Time marching
DG (conservative variables)	Lagrange	$3p + 1$	Roe's approximate Riemann solver with entropy fix [5]	Conservative	RK4
DG (entropy variables)	Lagrange	$3p + 1$	Roe's approximate Riemann solver with entropy fix [5]	Entropy	RK4
Energy-stable SBP	N/A	Omega [3]	SATs with Roe flux [5]	Conservative	RK4
Entropy-stable SBP	N/A	Omega [3], Chan's dense-coupling [1]	SATs and volumetric flux terms with entropy-conservative flux by Ismail and Roe [4]	Conservative	RK4

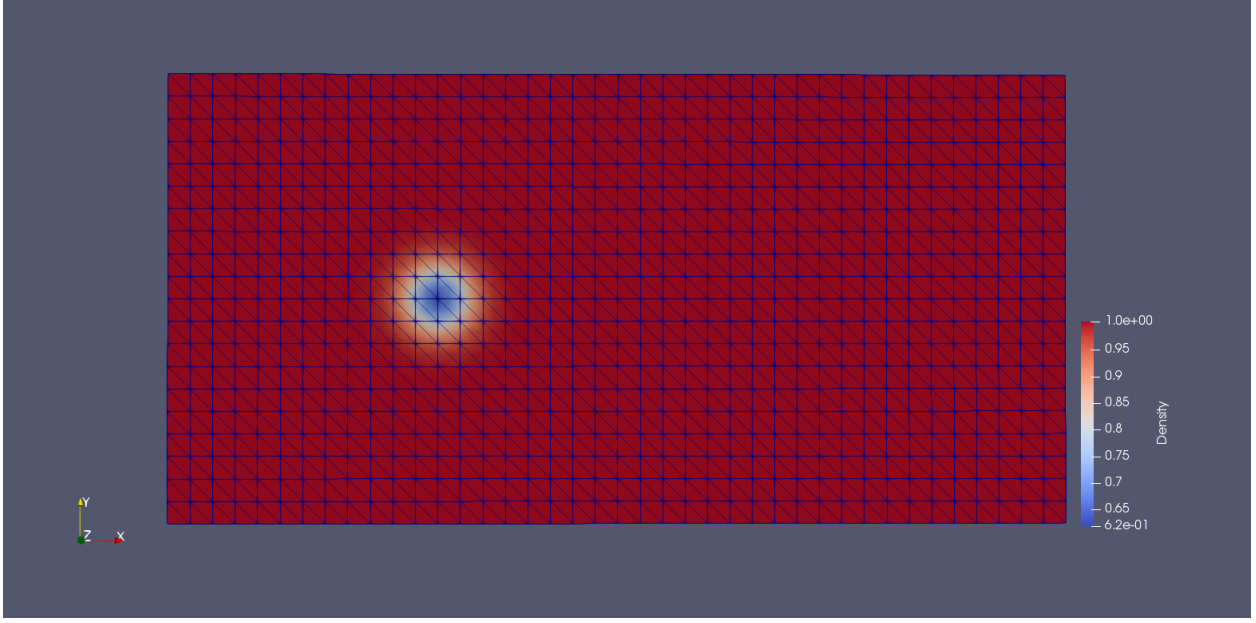


Figure 1: Mesh used to numerically solve the isentropic vortex problem; the mesh is overlaid on top of the density ρ at $t = 0$

Four schemes with varying levels of theoretical guarantee of nonlinear stability were applied to this problem, including: i) the DG method based on conservative variables, ii) the DG method based on entropy variables, iii) energy-conservative SBP, and iv) entropy-conservative SBP. The details of the implementation of the above schemes are shown in Table 2. For the purpose of this report, the DG method based on conservative and entropy variables, respectively, are sometimes referred to as energy- and entropy-stable DG schemes. Note that the quadrature rule for the DG schemes ensures that polynomials up to degree $3p + 1$ are integrated exactly, using the fewest number of points as possible.

Each of the schemes utilize a triangular mesh as shown in Figure 1. The triangular mesh is derived from splitting square elements such that the resulting mesh consists of right triangles. Grid refinement is achieved by uniformly scaling down the sides of the triangular mesh.

3.3 Taylor-Green Vortex

The Taylor-Green vortex problem [7] is a three-dimensional test case that simulates the compressible inviscid flow equations with the following initial conditions

$$\rho = 1, u = \sin(x) \cos(y) \cos(z), v = -\cos(x) \sin(y) \cos(z), w = 0,$$

$$p = \frac{100}{\gamma} + \frac{1}{16} \left(\cos(2x) \cos(2z) + 2 \cos(2y) + 2 \cos(2x) + \cos(2y) \cos(2z) \right)$$

which decay into smaller eddies over time. It is a challenging test case for simulating inviscid flows and can be used to assess the stability of schemes in under-resolved flows [2].

Four different schemes were applied to this problem, including: i) the DG method based on conservative variables, ii) the DG method based on entropy variables, iii) energy-stable SBP, and iv) entropy-stable SBP. The problem is solved on the domain $[-\pi, \pi]^3$ with periodic boundary conditions from $t = 0$ to a final time of $t = 15$. The details of each of the four schemes can be found in Table 3. Note that, like the isentropic vortex test case, the quadrature rule of the DG schemes ensures exact integration for polynomials up to degree $3p + 1$.

Table 3: Implementation of energy- and entropy-stable DG and SBP schemes for the Taylor-Green vortex problem

Scheme	Basis functions	Quadrature/nodal distribution	Numerical flux	Variable type	Time marching
DG (conservative variables)	Legendre	$3p + 1$	Roe's approximate Riemann solver with entropy fix [5]	Conservative	RK4
DG (entropy variables)	Legendre	$3p + 1$	Roe's approximate Riemann solver with entropy fix [5]	Entropy	RK4
Energy-stable SBP	N/A	Omega [3]	SATs with Roe flux [5]	Conservative	RK4
Entropy-stable SBP	N/A	Omega [3], Chan's dense-coupling [1]	SATs and volumetric flux terms with entropy-conservative flux by Ismail and Roe [4]	Conservative	RK4

4 Results and Discussion

This section presents and discusses the results from the linear advection, isentropic vortex, and Taylor-Green vortex test cases. Comparisons of each of the schemes are made in terms of convergence, accuracy, and robustness.

4.1 Linear Advection

Table 4 shows the convergence rates of the DG and SBP schemes applied to the linear advection problem. A CFL number of 0.05 was used for all degrees except for $p = 4$, where 0.01 was used as the CFL condition to ensure that errors from the time stepping method were insignificant. Table 4 shows that all three schemes performed at the expected $p + 1$ convergence rate at all degrees except for $p = 1$ and $p = 4$. For $p = 1$, the SBP and DG schemes with upwind flux terms performed better than the expected $p + 1$ convergence rate, while for $p = 4$, the SBP scheme with symmetric flux terms performed more poorly than the expected rate.

Figure 2 shows the log-log plots of the error against the mesh spacing, where ‘mesh spacing’ refers to the size of the elements. The error is defined as $(\int_{\Omega} (u - u_h)^2 dx)^{1/2}$, where Ω refers to the domain and u and u_h are the analytical and numerical solutions, respectively. The same CFL values were used as Table 4. It can be seen that the absolute error decreased while the convergence rate increased with increasing the degree of the schemes, which is consistent with theory. Moreover, the DG and SBP schemes with upwind flux terms performed in a very similar manner in terms of the convergence rates and absolute error values. Note, however, that the DG scheme with upwind flux terms delivered reduced accuracy for the finest mesh considered in each case in Figure 2 (b)-(d). The reason for this has not been investigated.

Table 5 shows the maximum CFL values for which each of the schemes were stable. Here, stability was defined as a change in energy up to roughly $+10^{-7}$. This definition ensured that an increase in the CFL number beyond the quoted values would lead to an energy increase

Table 4: Convergence rates of $p = 1$ to $p = 4$ DG and SBP schemes applied to the linear advection problem with $CFL = 0.05$ for $p = 1, 2, 3$ and $CFL = 0.01$ for $p = 4$

p	DG (upwind flux)	SBP (upwind flux)	SBP (symmetric flux)
1	2.6898	2.7071	2.0011
2	3.0726	3.0491	3.0220
3	4.0102	3.9999	4.1312
4	5.0271	4.9631	4.6929

Table 5: Limiting CFL values for stability of DG and SBP schemes applied to the linear advection problem

p	DG (upwind flux)	SBP (upwind flux)	SBP (symmetric flux)
1	0.70	0.47	0.70
2	0.35	0.23	0.35
3	0.21	0.14	0.21
4	0.14	0.10	0.14

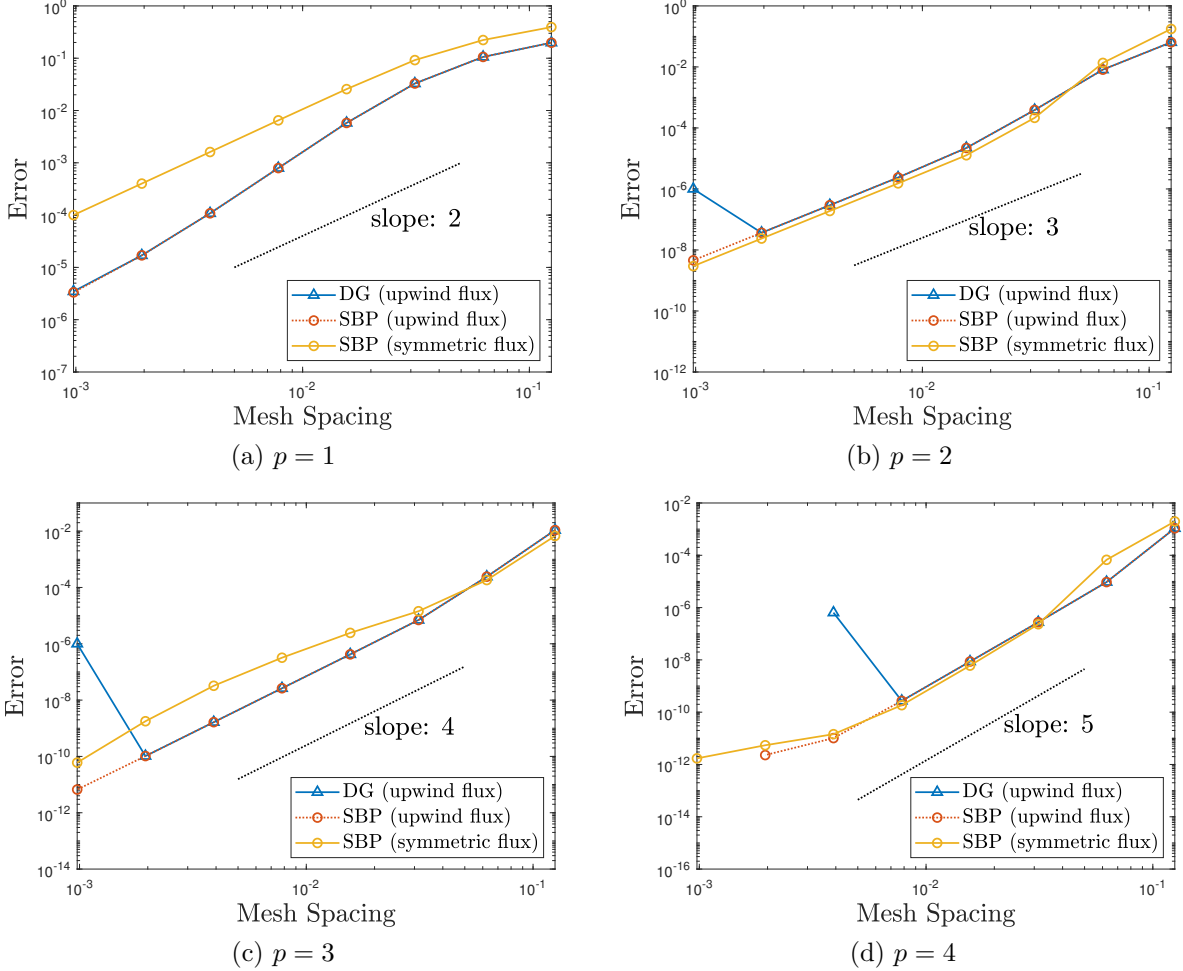


Figure 2: Convergence plots of $p = 1$ to $p = 4$ DG and SBP schemes applied to the linear advection problem

of $\pm\text{nan}$ or otherwise close to an unphysical, large value. We observe that as the degree of each of the scheme increased, the limiting CFL values decreased, implying that a smaller time step must be employed to ensure linear stability. Likewise, higher-order schemes may induce additional computational cost to meet stability requirements, despite that a coarser mesh may be used to deliver similar accuracy levels as lower-order methods, although the effect of the coarsened mesh on the computational cost generally far outweighs the effect of the reduced CFL number. In addition, we see that the DG method with upwind flux terms and SBP method with symmetric flux terms have noticeably higher limiting CFL values compared to the SBP method with upwind flux terms. Given that all three schemes are energy-conservative or energy-stable, this indicates that the DG method with upwind flux terms and SBP method with symmetric fluxes may be more favorable in terms of ensuring that energy-stability is met at lower computational cost.

Of all the energy-stable schemes that were studied, the DG scheme with upwind flux terms may be most favorable as it converges quickly while having the least stringent CFL requirements to ensure stability. It can also be seen that all three schemes have a trade-

off between convergence and maximum allowable CFL as the degree increases; higher-order schemes converge more quickly, but require smaller CFL values to ensure stability which can be costly.

4.2 Isentropic Vortex

Table 6 shows convergence rates of energy- and entropy-stable DG and SBP schemes of various degrees ($p = 1$ to $p = 4$). A log-log plot of the error of each of the four schemes is plotted against the mesh spacing in Figure 3. A CFL of 0.05 was used. ‘Mesh spacing’ in Figure 3 refers to the square root of twice the area of the triangular elements. Meanwhile, the error in Figure 3 is the sum of all $(\int_{\Omega} (x_i - x_{h,i})^2 dx)^{1/2}$ where x_i are the analytical solutions of u, v, ρ , and p and $x_{h,i}$ correspond to their numerical solutions.

It can be seen from both Table 6 and Figure 3 that the convergence rates of the four schemes increased with increasing p . Moreover, each of the schemes performed at the expected $p+1$ convergence rate, or greater, in the case of $p = 1$ and $p = 2$ schemes. No notable differences in the convergence of energy- and entropy-stable schemes were observed. Interestingly, the SBP schemes outperformed the DG schemes in terms of accuracy, obtaining numerical solutions with smaller absolute errors on multiple grids at orders from $p = 1$ to $p = 4$. This result is independent of the nodal distribution; the same result would arise even if the error was plotted against the number of degrees of freedom.

Table 6: Convergence rates of $p = 1$ to $p = 4$ energy- and entropy-stable DG and SBP schemes applied to the isentropic vortex problem with $\text{CFL} = 0.05$

p	DG (conservative variables)	DG (entropy variables)	energy-stable SBP	entropy-stable SBP
1	2.2958	2.4243	2.3252	2.4521
2	3.3184	3.3857	3.2657	3.1327
3	4.2022	4.1058	3.7786	3.8269
4	5.0568	4.9734	4.8613	4.9073

Table 7: Limiting CFL values for stability of energy- and entropy-stable DG and SBP schemes applied to the isentropic vortex problem

p	DG (conservative variables)	DG (energy variables)	energy-stable SBP	entropy-stable SBP
1	0.26	0.26	0.26	0.26
2	0.15	0.15	0.15	0.15
3	0.10	0.10	0.082	0.080
4	0.072	0.071	0.062	0.062

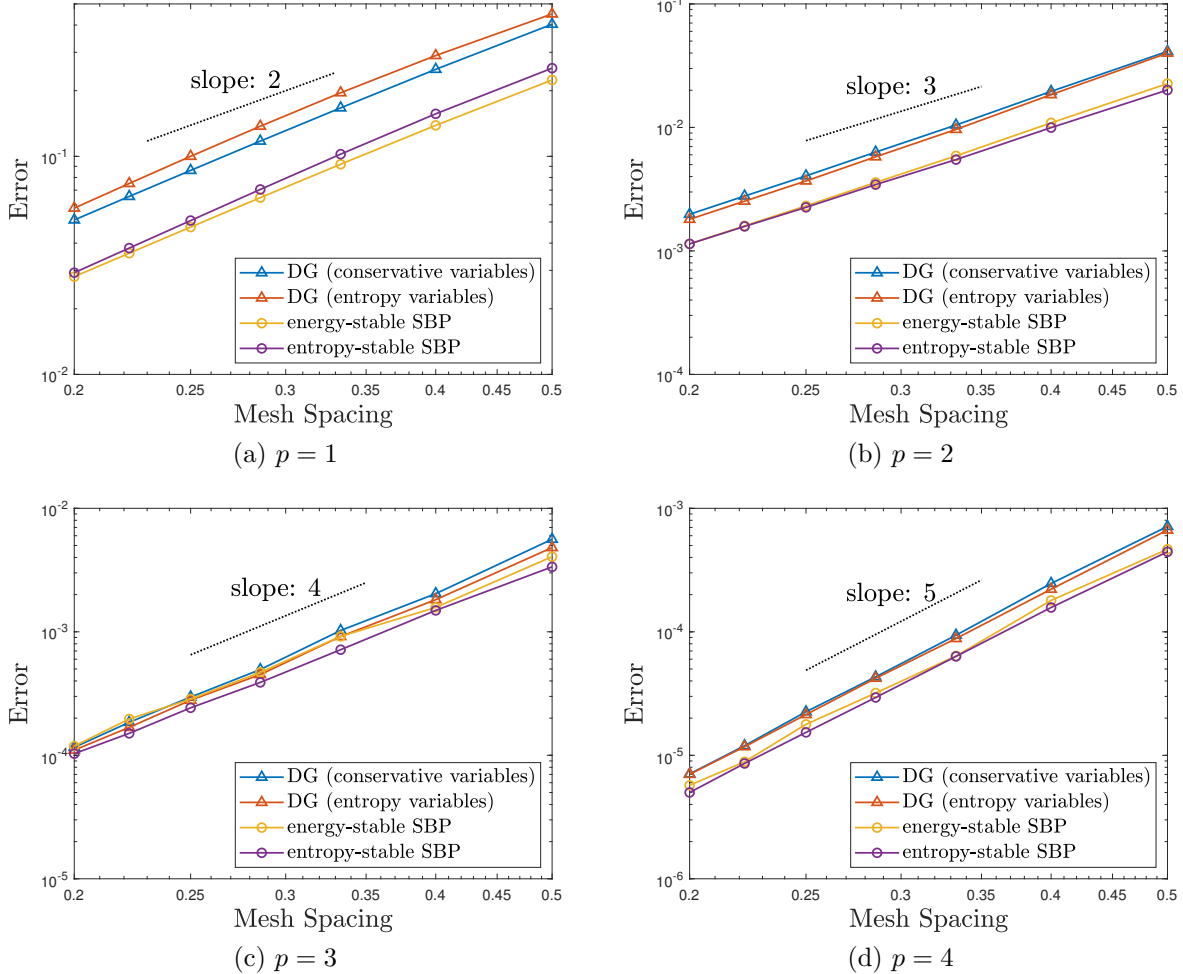


Figure 3: Convergence plots of $p = 1$ to $p = 4$ energy- and entropy-stable DG and SBP schemes applied to the isentropic vortex problem

Table 7 shows the maximum CFL values, in two significant figures, for which each of the schemes were stable. Similar to the linear advection problem, stability is defined as a change in entropy up to roughly $+10^{-7}$. Using this definition, the limiting CFL values for stability of the energy-stable DG and SBP schemes mirrored their counterparts (the entropy-stable DG and SBP schemes, respectively). Moreover, for $p = 3, 4$ the energy- and entropy-stable DG schemes outperformed the SBP schemes, allowing for larger time steps on a given mesh while maintaining stability.

If instability was defined as an increase in entropy by an amount larger than machine zero rather than an increase of $\pm nan$, the maximum allowable CFL number would be different. In particular, the energy-stable schemes would become unstable at lower CFL numbers than entropy-stable schemes with this new definition. An example of this is shown in Figure 4, where the entropy of energy-stable schemes increases by a finite amount over time with a CFL of 0.05, whereas it decreases for the entropy-stable schemes.

Overall, energy- and entropy-stability properties did not have a significant effect on the convergence or limiting CFL for stability when solving the isentropic vortex problem, indi-

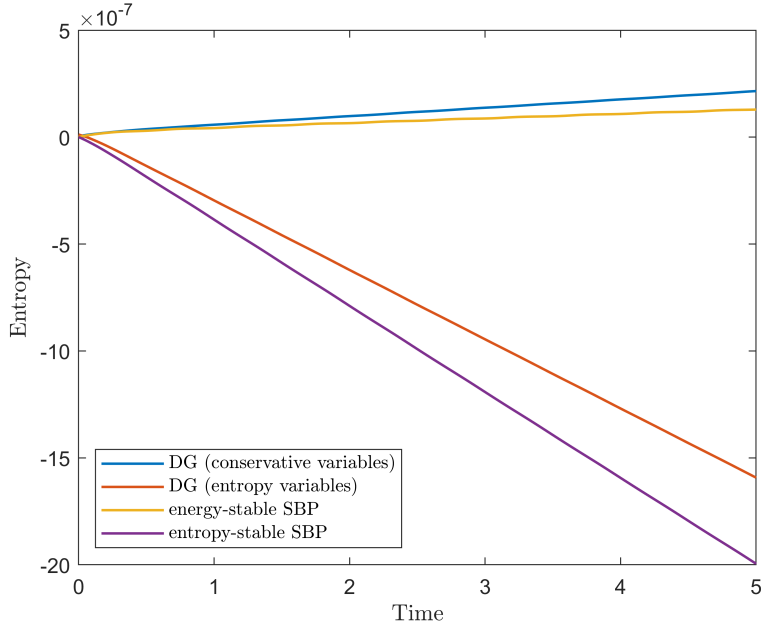


Figure 4: Evolution of entropy for $p = 4$ energy- and entropy-stable DG and SBP schemes at $\text{CFL} = 0.05$ for the isentropic vortex problem

cating that energy-stable schemes may be beneficial in this case, if they can be shown to be less computationally costly compared to entropy-stable schemes *a priori*. Furthermore, our results show that there is a potential trade-off between accuracy and the maximum allowable CFL value to ensure stability when it comes to choosing between DG and SBP schemes and choosing between multiple orders of the same scheme. Specifically, the DG schemes have less stringent time step requirements but have higher absolute error compared to the SBP schemes, whereas higher-order schemes deliver greater accuracy on the same mesh as lower order schemes, but have more stringent CFL requirements to ensure stability.

4.3 Taylor-Green Vortex

Since the Taylor-Green vortex problem does not have an analytical solution at $t > 0$, only the limiting CFL was studied for the energy- and entropy-stable DG and SBP schemes. Table 8 shows the maximum CFL values for which each of the schemes were stable. While interpreting the table, note the following:

- ‘–’ indicates that the test could not be completed within a 24-hour time frame
- ‘ $< x$ ’ indicates that the scheme was unstable for $\text{CFL} = x$, and that the limiting CFL value is smaller than x , but by an unknown amount
- the number of significant figures used for the CFL values is meaningful; for example, the entropy-stable DG scheme has a limiting CFL value of 0.08, but it could for instance be 0.085 if stated with two significant figures

Table 8: Limiting CFL values for stability of energy- and entropy-stable DG and SBP schemes applied to the Taylor-Green vortex problem

p	DG (conservative variables)	DG (entropy variables)	energy-stable SBP	entropy-stable SBP
1	0.8	0.08	0.80	0.085
2	–	–	< 0.001	0.045
3	–	–	0.35	0.02
4	–	–	< 0.001	< 0.01

Overall, our results show that odd-degree energy-stable SBP schemes have entropy-stable characteristics given that CFL requirements are met. In fact, odd-degree energy-stable SBP schemes are superior to odd-degree entropy-stable SBP schemes in terms of having less stringent CFL requirements to ensure nonlinear stability. As such, a larger time step can be applied with the energy-stable SBP scheme to ensure entropy-stability, which can reduce computational cost.

For even-degree SBP schemes, the entropy-stable schemes retain their theoretical advantage of nonlinear stability compared to energy-stable schemes. Even-degree energy-stable SBP schemes were found to be unstable even for very small CFL values.

Based on results that were collected so far for the energy- and entropy-stable DG schemes, the DG schemes appear to perform at a very similar level to their SBP counterparts. However, more results need to be collected before further assessment.

5 Conclusion

This study elucidated similarities and differences in the performance of energy- and entropy- stable schemes. For the isentropic vortex problem, energy- and entropy-stability properties were found to have no significant effect on the convergence rate or the limiting CFL for stability. However, for the Taylor-Green vortex problem, energy- and entropy-stability properties had noticeable consequences on the limiting CFL. Specifically, odd-degree energy-stable SBP schemes outperformed odd-degree entropy-stable SBP schemes with approximately ten-fold higher limiting CFL values. For even-degrees, entropy-stable schemes retained their theoretical advantage over energy-stable schemes.

This study also looked at similarities and differences in the performance of DG and SBP schemes. Between multiple energy-stable schemes applied to the linear advection problem, it was found that the DG scheme with upwind flux terms converged most quickly while having the least stringent CFL requirements. For the isentropic vortex problem, the DG schemes were found to have higher absolute errors than the SBP schemes but less stringent CFL requirements to ensure stability. Finally, for the Taylor-Green vortex problem, the DG and SBP schemes appeared to have similar limiting CFL numbers, but more testing must be done for verification.

In addition, this study compared the performance of higher-order schemes to lower-order

schemes. In general, we found a trade-off between accuracy, convergence rates, and the limiting CFL for stability. Specifically, as the degree of the schemes were increased, higher accuracy and convergence rates could be achieved at the cost of having more stringent CFL requirements for stability.

Given that our study only focused on limiting CFL values and accuracy to assess each of the schemes' performance, it would be interesting to also compare the computation time of each of the schemes by implementing them in a unified framework. It would also be interesting to test the Taylor-Green vortex case for degrees higher than $p = 4$ to see whether the differences between odd-even limiting CFL values hold in general. Additionally, it could be worthwhile to modify the implementation of the DG schemes for the Taylor-Green vortex problem and run the test cases for $p = 1$ to 3 until completion. Finally, assessing the performance of each of the schemes for other test cases may help us better understand the practical differences in each of the schemes.

6 Acknowledgements

First and foremost, I would like to thank Professors David W. Zingg and Masayuki Yano for giving me the opportunity to work with them and supporting me throughout this sixteen-week journey. Without their guidance and helpful discussions, this project would not have been possible. I also thank Siavosh Shadpey and Tristan Montoya who have helped me very closely with this project and shared their many insights. In addition, I would like to thank Professor Masayuki Yano for allowing me to use his Automated PDE Solver (APS) and Siavosh Shadpey for allowing me to use his driver files for my project. Last but not least, I would like to acknowledge the Natural Sciences and Engineering Research Council of Canada (NSERC) for funding me through the Undergraduate Student Research Awards program.

References

- [1] Jesse Chan. On discretely entropy conservative and entropy stable Discontinuous Galerkin methods. *Journal of Computational Physics*, 362:346–374, 2018.
- [2] Jared Crean, Jason E Hicken, David C Del Rey Fernández, David W Zingg, and Mark H Carpenter. Entropy-stable Summation-by-Parts discretization of the euler equations on general curved elements. *Journal of Computational Physics*, 356:410–438, 2018.
- [3] Jason E Hicken, David C Del Rey Fernández, and David W Zingg. Simultaneous approximation terms for multidimensional Summation-by-Parts operators. In *46th AIAA Fluid Dynamics Conference*, 2016 3971.
- [4] Farzad Ismail and Philip L Roe. Affordable, entropy-consistent Euler flux functions ii: Entropy production at shocks. *Journal of Computational Physics*, 228:5410–5436, 2009.
- [5] Philip L Roe. Approximate Riemann solvers, parameter vectors, and difference schemes. *Journal of computational physics*, 43(2):357–372, 1981.
- [6] Siavosh Shadpey and David W Zingg. Energy-and entropy-stable multidimensional Summation-by-Parts discretizations on non-conforming grids. In *AIAA Aviation 2019 Forum*, 2019 3204.
- [7] Geoffrey Ingram Taylor and Albert Edward Green. Mechanism of the production of small eddies from large ones. *Proceedings of the Royal Society of London. Series A-Mathematical and Physical Sciences*, 158(895):499–521, 1937.
- [8] Zhijian J Wang, Krzysztof Fidkowski, Rémi Abgrall, Francesco Bassi, Doru Caraeni, Andrew Cary, Herman Deconinck, Ralf Hartmann, Koen Hillewaert, Hung T Huynh, et al. High-order CFD methods: current status and perspective. *International Journal for Numerical Methods in Fluids*, 72(8):811–845, 2013.